BEAM INTERACTION WITH THIN MATERIALS: HEAT DEPOSITION, COOLING PHENOMENA AND DAMAGE LIMITS

M. Sapinski *, CERN, Geneva, Switzerland

Abstract

Thin targets, inserted into particle beams can serve various purposes, starting from beam emittance measurements like in wire scanner or scintillating screens up to beam content modifications like in case of stripper foils. The mechanisms of energy deposition in a thin target for various beam types are discussed, together with properties of particles produced in this kind of interaction. The cooldown processes, from heat transfer up to cooling by sublimation, and their efficiencies are presented. Finally, damage conditions are discussed and conclusions about typical damage limits are drawn. The experiments performed with the wire scanners at CERN accelerators and a mathematical model of heating and cooling of a wire are presented.

INTRODUCTION

The alpha scattering experiment, performed by Ernest Rutheford's students, Hans Geiger and Ernest Marsden, changed our understanding of matter. It was one of the first experiments with a particle beam hitting a thin target.

A century later the interaction of the beam with a thin target remains an important tool in many fields of science and technology. Here only a small part of this broad subject, related to the beam instrumentation, is covered. The paper is additionally biased because author is involved in wire scanners on high-energy hadron beams.

ENERGY DEPOSIT FROM DIRECT BEAM INTERACTION

The Bethe-Bloch formula, which describes the interaction of heavy charged particles with material, is shown in Equation 1.

$$-\frac{dE}{dx} = K z^2 \frac{Z}{A} \frac{1}{\beta^2} \left(\frac{1}{2} ln \frac{2m_e (c\beta\gamma)^2 T_{max}}{I^2} - \beta^2 - \frac{\delta}{2} \right)$$

(1)

where $K = \frac{4\pi e^4 N_A}{m_e c^2}$ (in CGS system), I is mean excitation energy of the target material, T_{max} is maximum energy transfer in a single collision, and δ is a density correction.

For particles of typical energies the Bethe-Bloch equation is visualized in Fig. 1. There are four main features visible on these curves:

- for $\beta\gamma \lesssim 3$ the energy loss decrease following $\beta^{-5/2}$ function is driven by the time the particles spend interacting with the electrons in the material;

- for $\beta\gamma \approx 3$ there is a minimum of energy loss in the material (MIP);
- for $\beta\gamma > 3$ but $\beta\gamma \lesssim 100$ a relativistic rise due to Lorentz transformation of transverse electric field intensity is observed;
- for $\beta\gamma > 100$ a density correction i.e. screening the electric field of projectile due to polarization of the material, shields the effective range of interactions and saturates the relativistic rise behaviour;
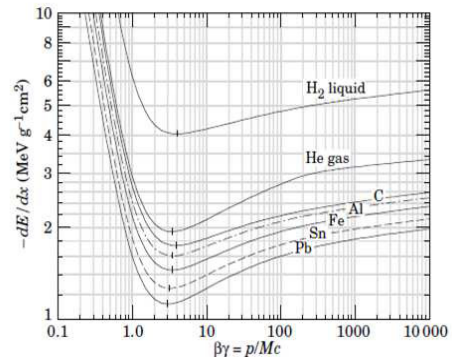

Figure 1: dE/dx for heavy particle crossing matter [1].

Geant4 simulations of energy deposition of 7 TeV protons in 33 μm carbon fiber is shown in Fig. 2. The main part of the energy deposition is due to the electronic energy loss which is fitted by a Landau curve. The high-energy tail of the Landau curve is cut due to knock-on electrons which have enough energy to leave the target, therefore not contributing to the energy deposit. The inelastic interactions are represented by a gaussian curve with mean value of about 3 MeV. Because of the small inelastic cross section of about 200 mbarn, the contribution of these events to the total energy deposit is below 1%.

The high-energy electrons lose energy in materials mainly through radiative losses, but for thin targets the energy deposition is similar as for charged hadrons. The ions are expected to deposit significantly more energy than protons due to z^2 component in Equation 1.

RF Heating

In 1990s the wire breakage without scanning the beam was observed at LEP. An investigation with a CCD camera revealed that the wire was hot mostly at the extremities, as can be seen in Fig. 2. This temperature pattern was attributed to RF coupling of the wire to the beam field.

In order to minimize the RF coupling the wire scanner tank has been redesigned to generate fewer wakefields. In
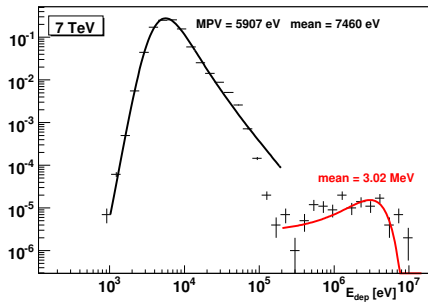
---

* mariusz.sapinski@cern.ch

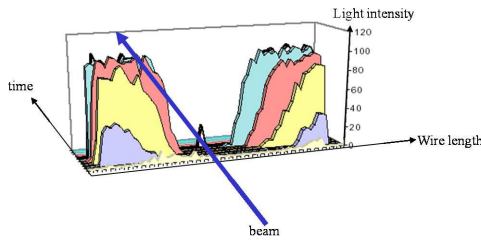Figure 2: Distribution of 7 TeV proton energy deposit in carbon fiber.

Figure 3: Pattern of RF heating of a $8\ \mu m$ carbon fiber in the LEP wire scanner [2].

the LHC case [3] ferrites were installed in the tank to suppress the build-up of RF modes and the RF heating is small compared to the direct beam interaction.

DAMAGE MECHANISMS

The mechanisms which lead to the target damage could be:

- mechanical failure (brittle or plastic);
- thermal shock;
- electrical discharges;
- radiation damage;
- thermo-mechanical fatigue;
- sublimation/melting;

The actual damage is usually a composition of two or more of above mechanisms, for instance the thermo-mechanical fatigue leads to decrease of the mechanical strength of the wire and then to a mechanical failure. If the target breaks because of mechanical failure or thermal shock at the very first beam, then probably the setup was wrongly designed. The same is valid in case of electrical discharges. On the other hand the radiation damage and thermo-mechanical fatigue are long-term damage mechanisms which in principle cannot be avoided. The sublimation and melting processes often determine the actual limit of beam brilliance for the use of a given target.

COOLING MODEL

The evolution of temperature of a wire piece during the time dt can be described by Equation 3 (RF heating is ne-

glected):

$$
\begin{aligned}
\mathrm{E_{dep}}\frac{\mathrm{dN_{hits}}}{\mathrm{dt}} \ =\ & \rho_{\mathrm{C}}\mathrm{Vc_p(T)}\frac{\mathrm{dT}}{\mathrm{dt}} - \lambda(\mathrm{T})\mathrm{A_d}\frac{\mathrm{dT}}{\mathrm{dy}} \quad (2)\\
- \ & \mathrm{A_{rad}}\epsilon\sigma(\mathrm{T}^4 - \mathrm{T}_{amb}^4) - \Delta\mathrm{H_{sub}}\frac{\mathrm{dn}}{\mathrm{dt}}\\
- \ & \mathrm{A_{rad}}(\phi + \frac{2\mathrm{k_BT}}{\mathrm{q_e}})\mathrm{j_{th}}
\end{aligned}
$$

The contributions to the cooling are discussed in the following sub-sections.

Heat Capacity

The heat capacity of a material typically raises with the temperature. For the graphite, it raises from about $1\ \mathrm{J/g\cdot K}$ at room temperature to about $2.2\ \mathrm{J/g\cdot K}$ at 2700 K.

Materials with higher heat capacity usually have also higher density therefore the beam energy deposition is higher. This, as well as melting/sublimating temperature must be considered when choosing the optimal material for the target.

Conductive Cooling

Conductive cooling is described by Fourier law, which describes the energy transfer rate. In one-dimensional case it takes the form of Equation 3.

$$
P_{cool}^{cond} = -\lambda(T)A_d\frac{dT}{dx} \quad (3)
$$

where $\lambda(T)$ is thermal conductivity and A_d is surface of the target cross section, which is small because a thin target is considered. In case of graphite the thermal conductivity is about $1\ \mathrm{W/cm^2\cdot K}$ and decreases with temperature. Advanced materials like nanotubes are reported to have thermal conductivity almost 400 times larger than graphite.

Radiative Cooling

Radiative cooling is described by Stefan-Boltzmann law:

$$
P_{cool}^{rad} = A_{rad}\epsilon\sigma(T^4 - T_{env}^4) \quad (4)
$$

where A_{rad} is external surface of the sample, σ is Stefan-Boltzmann constant and ϵ is emissivity ($\epsilon = 1$ corresponds to black-body radiation). Radiative cooling is a surface effect, so it is more efficient for thinner targets, where ratio of surface to volume is larger.

Thermionic Cooling

Thermionic emission is an emission of electrons from the surface of a hot body. The density of emitted current is described by Equation 5:

$$
j_{th} = A_R T^2 exp(-\frac{\phi}{k_B T})(1 - R) \quad (5)
$$

where A_R is Richardson constant, ϕ - work function and k_B - Boltzmann constant. R represents a fraction of

electrons which come back to the emitting surface, therefore not participating in cooling (it is small for a thin fiber, but maybe important for a foil). The cooling power is expressed by Equation 6:

$$P_{cool}^{th} = A_{rad}(\phi + \frac{2k_B T}{q})j_{th} \qquad (6)$$

Materials with smaller work function have a better thermionic cooling. Placing a body in a strong electric field decreases its work function and could be used to enhance cooling. The current replacing electrons removed by thermionic emission lead to reheating of the body, but this effect is typically much smaller than the cooling.

Comparison of Cooling Processes

In a typical case of a carbon fiber the contribution of cooling processes to the total cooling is shown in Fig. 4 as a function of the fibre temperature. Radiative cooling dominates over large temperature range, but for temperatures above 3300 K the thermionic emission takes over.
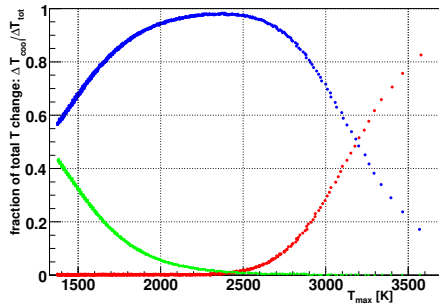
Figure 4: Comparison of cooling processes: contribution of thermionic (red curve), radiative (blue curve) and conductive (gren curve) cooling power to the total cooling as a function of carbon fibre temperature.

SUBLIMATION

The material behaviour in high temperatures and in a vacuum can be read from a phase diagram. Materials which sublimate under these conditions have an advantage because the sublimation temperature and sublimation heat are higher than melting temperature and heat.

Two sublimation models have been considered in this study. First asumes existence of a thin vapour layer around the target, being in the equilibrum with the target material [4]. Second model [5] is described by Equation 7.

$$logW[\frac{g}{cm^2 s}] = 12.04 - 0.5logT - \frac{4 \cdot 10^4}{T} \qquad (7)$$

Application of this model to the wire thermal model 3 leads to relatively good estimate of the amount of sublimated target material. In Figure 5 the evolution of the wire temparature during a scan of the beam is shown together with decrease of the wire diameter due to sublimation.
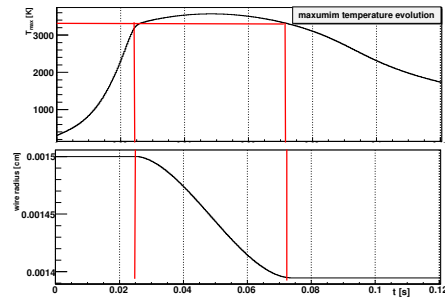
Figure 5: Evolution of the temperature of a wire (upper plot) and wire radius decrease (bottom plot) during scan of the beam in extreme conditions.

Sublimation Cooling

Sublimation removes the hottest fraction of the material from the surface, what is equivalent to a cooling, which is weak in comparison to other cooling processes. In case of graphite the vaporization heat is about 356 kJ/mole.

SECONDARY PARTICLES

The spectrum of secondary particles, shown in Fig. 6 is dominated by knock-on electrons. The higher-energy component is due to inelastic interactions. These particles are mainly photons and pions with multi-GeV energies.
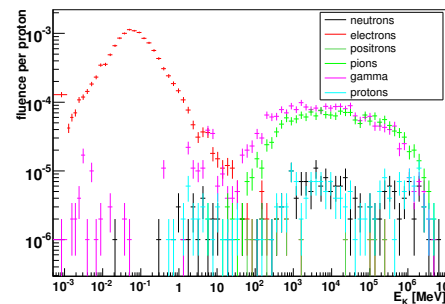
Figure 6: Spectrum of secondary particles generated by 7 TeV protons on $33\ \mu m$ carbon target.

RADIATION DAMAGE

The radiation damage is created when atoms are removed from their position in the lattice. The defect consists of an interstitial atom and a vacancy. To estimate the amount of displacements per atom (DPA) during a wire scanner lifetime the program SRIM [6] has been used. For a typical number of scans (10^4) the radiation damage is less 0.01 DPA. This damage is not expected to modify mechanical properties of the fiber. Therefore the long-term fiber damage is due to thermo-mechanical fatigue of the fiber material.

EXPERIMENTAL RESULTS

Five wire-breakage experiments performed at CERN are described here. They all use the same $33~\mu m$ carbon fiber, brought to CERN from Los Alamos in 1979. The properties of this fiber are not well known. The conditions for experiments described below are summarized in Table 1, where σ_t is beam size perpendicular to the scan direction.

1988 Experiment

One of the first wire breakage experiments was conducted on SPS beam with rotational scanner in 1988. The breakage took place at $10~\mathrm{cm/s}$. The evaluation of the cooling simulation for this experiment can be found in [7].

2008 Experiment

Two wire breakage experiments were performed in 2008 on SPS rotational scanners [8, 9]. The scan speed slowed down from 6 to 0.5 m/s. The wire had been gradually weakened by this sequence of scans which is taken into account in the calculation of sublimation.

A special beam cycle on the SPS has been prepared for this test. Beam intensity reached $2.4 \cdot 10^{13}$ circulating protons. In order to diminish the effect from RF-coupling the beam has been debunched. The beam transverse profiles have been close to Gaussian in both directions.
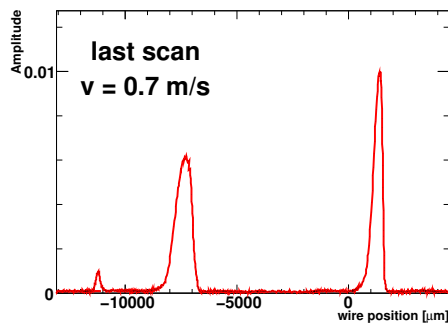

Figure 7: The last profile before the wire broke. The plot shows breakage of the horizontal wire: multiple peaks suggest that the wire was already fragmented.

In Fig. 7 the beam profile registered during the last scan of the horizontal scanner is shown. The multiple peaks are symptoms of the wire fragmentation. After the experiment the wire scanners were opened and both wires were photographed with scanning electron microscope. The images obtained with 1000 times magnification are shown for two positions: at the center of the beam impact, and 1 mm away (Fig. 8). They show that the main process deteriorating the wire is sublimation due to the high temperature. In the location of the fracture the remaining wire diameter is only about $7.5~\mu m$, which corresponds to the sublimation of 95% of the material. Finally the wire could not withstand mechanical forces during the scan. At 1 mm from the beam center the fiber is intact.
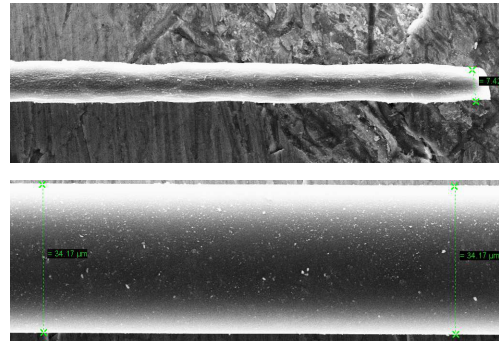
Figure 8: Fiber fracture at beam impact center (upper plot) and untouched fiber 1 mm away (bottom plot).

2010 Experiment

The experiment was performed on 2010 using the horizontal wire scanner installed on beam 2 of LHC [10]. It was devoted to investigation of quench limit for milisecond-duration losses.

The beam intensity was $1.53 \cdot 10^{13}$ protons and the energy was 3.5 TeV. The LHC scanners are linear devices with a nominal speed of 1 m/s. During the experiment the speed of the scan was gradually decreased down to $5~\mathrm{cm/s}$, when the magnet quenched. Technical problems with the wire scanner electronics were encountered which led to the loss of beam profile data for slow scans, but the magnet quench triggered an acquisition of BLM post-mortem buffers with high-precision data which are presented in Fig. 9.
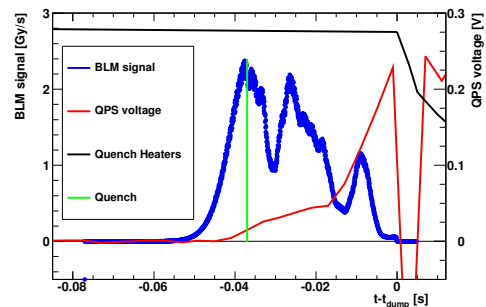

Figure 9: BLM post-mortem signals (blue) overlaid with QPS voltage readout (red) during the wire scan which led to quench of MBRB magnet. In the moment when quench heaters fire (black line, arbitrary units) the QPS reading is suffering from interference (gap in the data). The green line marks the time at which the QPS voltage indicates the presence of the resistive zone.

After the test the wire was inspected using a scanning electron microscope. At the location of the beam impact the wire material sublimated reducing its diameter by almost 50%, from $33~\mu m$ down to about $18~\mu m$ (Fig. 10). The linear charge density during the last scan was about 2 times larger than during the wire breaking in SPS.
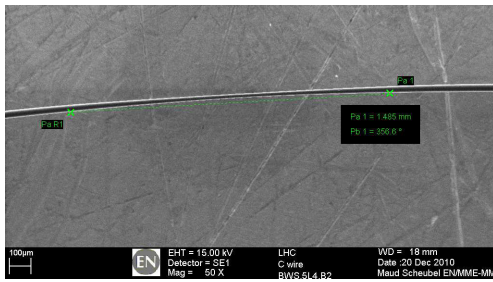
Figure 10: The carbon fiber after the experiment pictured using scanning electron microscope with magnification 50.

2011 Experiment

In 2011 a breakage with ion beam has been tested in the SPS. A horizontal linear scanner was chosen for this exercise. Pb^{82+} ions are expected to deposit much more energy in the fiber than protons (z^2 dependence in Equation 1). It was therefore unexpected that the fiber remained unbroken down to speed of 2 cm/s.

After the wire removal it has been found broken and electron microscope analysis revealed sublimation of the wire material down to about $4~\mu$m. The fracture can be seen in Fig. 11.
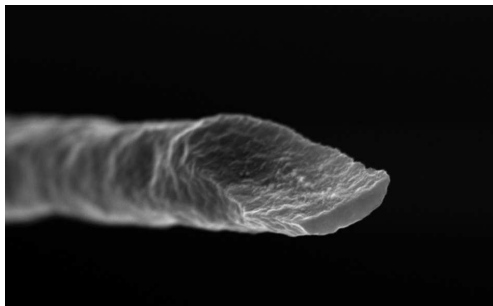

Figure 11: The carbon fiber after the experiment with ions.

Comparison of Experiments

The experimental conditions at which the carbon fibers were broken or significantly damaged are summarized in Table 1. It can be assumed that the wire breakage should depend on the density of charges traversing the wire:

$$n_{ch} = \frac{N_{ch}d_w}{v_w t_{rev}\sigma_t} \qquad (8)$$

The results are not easy to interpret. The first breakage occured for tough conditions. The two subsequent breakages are consistent, but the next experiment, on LHC, took place at more harsh conditions and the wire was only sublimated in 50% of diameter. The biggest surprise is the last result, where ions were used. According to Bethe-Bloch equation the charge density should be multipiled by 82^2, which gives 6000 times larger energy deposition than in case of tests with protons.

Table 1: Summary of Beam Conditions at Wire Breakage for All Discussed Experiments.

scan speed	N_{ch}	t_{rev} [μs]	σ_t [mm]	n_{ch} [mm^{-1}]
0.1 m/s	$2.0 \cdot 10^{13}$	23	0.73	$37 \cdot 10^{13}$
0.5 m/s	$2.4 \cdot 10^{13}$	23	0.73	$8.6 \cdot 10^{13}$
0.7 m/s	$2.2 \cdot 10^{13}$	23	0.57	$7.2 \cdot 10^{13}$
5 cm/s	$1.5 \cdot 10^{13}$	89	0.6	$17 \cdot 10^{13}$
2 cm/s	$2.6 \cdot 10^{11}$ (Pb)	23	0.6	$2.8 \cdot 10^{13}$

SUMMARY

In this paper the most important aspects of particle beam interactions with thin layer of material are discussed. The beam energy deposition, beam-target RF coupling and cooling mechanisms are described. A mathematical model, assessing the temperature evolution during exposition to the beam, is presented. In the cases discussed the sublimation of the target material is driving the short-term target performance, i.e. the most extreme conditions in which the target can be used.

The damage experiments performed at CERN in the last years are described, together with post-mortem analysis of the samples. Excluding the Pb^{82+} experiment, the linear charge density in damaging conditions varies by factor 5.

A lot can still to be done in terms of material choice and better understanding of the thermal and damage processes. Further investigations and experiments are planned.

REFERENCES

[1] K. Nakamura et al.(Particle Data Group), J. Phys G 37 075021 (2010), http://pdg.lbl.gov

[2] C. Fisher, R. Jung, J. Koopman, "Quartz wires versus carbon fibres for improved beam handling capacity of the LEP wire scanners", proceedings of BIW 1996.

[3] M. Sapinski, T. Kroyer, "Operational limits of wire scanners on LHC beams", proceedings of BIW 2008.

[4] P. Thieberger, "Upper Limits for Sublimation Losses from Hot Carbon Targets in Vacuum and in Gasses", MUC-0186, BNL

[5] S. Dushman, *Scientific foundations of vacuum technique*, Wiley Inc., New York (1966).

[6] J. Ziegler, J. Biersack, and U. Littmark, *The Stopping and Range of Ions in Solids*, Pergamon Press, New York (1985).

[7] M. Sapinski,"Model of Carbon Wire Heating in Accelerator Beam", CERN-AB-2008-030-BI

[8] M. Sapinski, B. Dehning, A. Guerrero, J. Koopman, E. Metral, "Carbon Fiber Damage in Accelerator Beam", CERN-BE-2009-028, proceedings of DIPAC09

[9] M. Sapinski et al., "Carbon Fiber Damage in Particle Beam", CERN-BE-2011-003, proceedings of HB2010

[10] M. Sapinski et al.,"LHC Magnet Quench Test with Beam Loss Generated by Wire Scan", CERN-ATS-2011-062, proceedings of IPAC2011